Robust Thresholding by Calibration

Zhenzhou Wang
Shenyang Institute of Automation,
Chinese Academy of Sciences
Shenyang, P.R. China
wangzhenzhou@sia.cn

***Abstract*—Although image segmentation technology has achieved rapid development, threshold method is still an indispensable part in many practical applications. The most advanced methods do not perform well in the segmentation of many different types of images. Therefore, it is expected that the optimal segmentation method can be obtained for images with different modalities. In this paper, a robust threshold method is proposed to calibrate the parameters to obtain the best accuracy. The proposed threshold method is tested in the composite image and the actual image. The experimental results show that the proposed method is superior to the existing technology.**

Keywords—Segmentation; Thresholding; Image Processing; slope difference distribution.

I. INTRODUCTION

Image segmentation has been extensively studied for decades, and its application is widely used in different visual applications. After a long time, the analysis remains challenging, and the researchers turn their attention to advanced algorithms. Although the research enthusiasm of threshold selection has been greatly reduced, threshold selection as the basic technology of image segmentation is still an important part of image processing application. Over the past several decades, many threshold selection methods have been proposed [1-21], which are based on different computational criteria. We divide the most advanced threshold selection methods into the following categories. (1) Histogram based Entropy computation method [2-3]; (2) Iteration based method [4]. (3) Histogram based modeling method [5-13]; (4) Histogram profile based method [14]; (5) Fuzzy method [15-21]. Based on the entropy method, the optimal threshold value is calculated by selecting the maximum entropy information of the segmented histogram distribution. Different researchers [1] have proposed different algorithms to calculate the entropy, and its performance varies according to the shape of the image. For fuzzy images, different membership functions are proposed and the optimal threshold is calculated by combining entropy function [1]. Their performance varies from the mode of the image to be divided [1]. The iterative method can find the threshold by convergence, and its performance is changed by the mode of the segmented image [4]. Based on the modeling method, the criterion to be derived from the proposed model is maximized. For example, Otsu proposed a popular model in 1979, which is still one of the most commonly used threshold selection methods today. Similar to the entropy based approach, the modeling approach also finds the threshold from global optimization. Most models assume that the gray-scale distribution of Gaussian distribution is two classes. For the histogram profile based method, [14] uses convex hull method to find the concave position as a candidate for threshold. However, the threshold is easily trapped in the local valley, not the global valley. In some cases, there is no valley at all in histogram distribution. For the fuzzy method [15-19], different membership functions, such as class II fuzzy set [15, 16] and fuzzy C-means [19] are proposed to divide the pixel class. These methods based on fuzzy sets have become very popular with existing technology methods because of their good performance. There is only one common background in these threshold selection methods, which are based on image histogram. In addition, there are other popular segmentation methods that share common ground with threshold selection methods, for example, clustering based methods [20-25] are very popular in actual image segmentation applications. For example, in MR image segmentation, cell clustering based on fuzzy sets is usually used in [20-22], expectation maximization (EM) based clustering [23], k-means based clustering [24] and non-convex model based clustering [25] and other application specific image. In our experiments, these most advanced methods often make mistakes when providing segmentation solutions.

In this paper, a robust threshold method is proposed based on the slope difference distribution of image histogram. The slope differential (SD) distribution is used to cluster and divide the different pixel classes. The peak value of slope difference distribution corresponds to the average of different pixel categories, and the valley value of slope difference is corresponding to the threshold point between different pixel categories. In order to quantitatively evaluate and compare the existing technical methods, the threshold selection method is tested for different types of composite images with different noise sizes. In addition, we also tested the proposed methods using the actual image of different modalities obtained from different applications, for example, the left ventricle MR images, microscope images and welding laser line images. The experimental results show that the proposed threshold selection method is better than the existing technology in different image segmentation.

The organizational structure of this article is as follows. Firstly, the proposed threshold selection method is described in section 2. In section 3, the advantage of the proposed threshold selection method over the state of the art segmentation method is to test with the actual image and the composite image. Qualitative results show that the proposed method is superior to the existing method in segmentation precision. We conclude in section 4.

978-1-5386-1127-2/17/$31.00 ©2017 IEEE

II. PROPOSED METHOD

The proposed threshold selection algorithm consists of the following three parts: (1) calculate the slope difference distribution based on normalized image histogram; (2) select the threshold according to the calculated slope distribution peak valley; (3) calibrate parameters to produce optimal segmentation accuracy. This section describes all three sections in detail.

A. Slope difference distribution

Image histogram is the pixel distribution in the image. We define the slope distribution of the image as the rate of change of the pixel distribution [31].

First, we rearrange the gray value of the image according to the interval range [1, 255] and calculate its normalized histogram distribution $P(x)$. Secondly, we use the discrete Fourier transform (DFT) low-pass filter to filter the normalized histogram distribution in the frequency domain. The DFT filter bandwidth is 10. We calculate two slopes for each point of the point on $P'(x)$, one on the left side and the other on the right side. We calculate them based on a line model at N adjacent points of each side. This parameter $N_{fitting}$ needs to be calibrated.

B. Thresholding

According to the segmentation requirement, the proposed threshold selection process is flexible and has some variable manual input. The number $N_{fitting}$ is the first manual input, which is fitting points of the line model and its default value is 15. The number of pixel classes is the second manual input, which is the image contains and its default value is 2. The case C is the third manual input, in which the user wants the image to be segmented. According to attribute 1, the number of pixels is determined by the number of peaks, N_{peak} of the slope difference distribution and the value of N_{peak} should be at least 2. However, not all peaks can be used to segment the image into significant regions. According to the reduction direction to classify the peak, the pixel value of the classification peak is defined as the mean of pixel level, 1, 2, 3, 4, etc. Case C =1 (the default value) is used for segmenting between pixel class 1 and pixel class 2. Case C =2 is used for segmenting between pixel class 2 and pixel class3. Case C =3 is used for segmenting between pixel class 3 and pixel class 4. The other cases, C =5, 6, 7 and so on are the same definition. The valley value of the maximum absolute value between the two peak values of the two pixel categories to be segmented is found, and we select the pixel value of the valley as the segmentation threshold. It can be seen that the number of the valleys N_{valley} in the slope difference distribution should be at least 1. Algorithm 1 describes the procedure of selecting the threshold value.

Algorithm 1 The threshold selection process

Input: Image, I with grayscale values re-arranged in the interval [0, 255]; The number of fitting points of the line model, $N_{fitting}$; The number of pixel classes, $N_{classes}$; The case in which the user wants the image to be segmented, C.

Output: The selected threshold T

Initialization:

1) Calculate the normalized histogram of the input image and smoothing the normalized histogram with the filter based on the Fourier transform.
2) Calculate the slope difference distribution.

Threshold selection:

3) Order the peak value of the slope difference distribution in the direction of reduction.
4) Select the first $N_{classes}$ peaks as an effective peak and delete other smaller peaks.
5) Choose two peaks according to the input case and locate the maximum absolute value of the valley.
6) Select the threshold for the location of the valley corresponding to the find, V_i.

Result: the threshold $T = V_i$.

C. Calibration

Algorithm 2 describes the procedure of calibration.

Algorithm 2 The calibration process

Input: A typical image, I selected from a specific type of images with grayscale values re-arranged in the interval [0, 255]; The known segmentation result, S_{ideal} for the inputted image; The number of pixel classes, $N_{classes}$; The case in which the user wants the image to be segmented, C.

Output: The number of fitting points of the line model, $N_{fitting}$ for this specific type of images;

Initialization:

1) Calculate the normalized histogram of the input image and smoothing the normalized histogram with the filter based on the Fourier transform

for N = 5,6, …, 59, 60

Segmentation:

2) Compute the slope difference distribution.
3) Order the peak value of the slope difference distribution in the direction of reduction.
4) Select the first $N_{classes}$ peaks as an effective peak and delete other smaller peaks.
5) Choose two peaks according to the input case and locate the maximum absolute value of the valley.
6) Select the threshold for the location of the valley corresponding to the find, V_i.
7) Obtain the segmentation result, S_t with the selected threshold.

Calibration:

8) Compute the F-measure between S_t and S_{ideal}.

end;

Results: Select the N that yields the largest F-measure as $N_{fitting}$.

III. Experimental Results and Discussion

A. Experimental Results

To verify that the proposed threshold selection method is more advantageous than the existing technology segmentation method, we use the image containing four linear objects as the test pattern. The background gray average is 40, two vertical objects are 90 and 140, the left horizontal object is 180 and the right horizontal object is 230. The variance of Gaussian noise is equal to 30. We compare the proposed threshold selection method with ACNE [26], RAC [27], DRLS [28], NC [30], TSCE [1], TEFE [1], ITS [1], TSME [1], Otsu [5], STS [18], FCM [19], GM, EM [23] and KM [24]. Fig. 1 (a) shows the synthesized image and the segmentation results are shown in Fig. 1 (b)-(p). It can be see that only the proposed threshold selection method, K-means method and EM method can completely separate objects from the background. In contrast, the result of EM method is over-segmented and the result of K-means is under-segmented. *Please note that we did not calibrate the parameter N in this specific example and the default value 15 is used.*

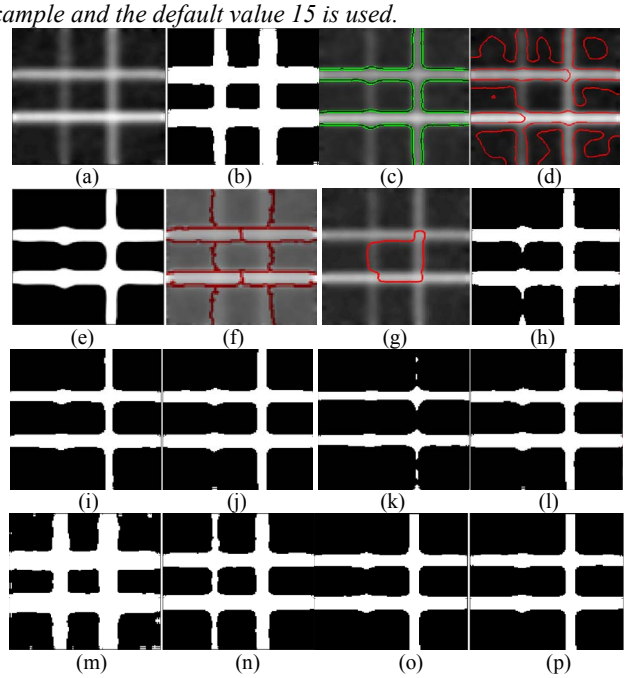

Fig. 1. Comparing SD-threshold selection method with state of the art segmentation methods (a) The synthesized image; (b) Segmentation result by the proposed SD-threshold selection method; (c) Segmentation result by ACNE; (d) Segmentation result by RAC; (e) Segmentation result by GM; (f) Segmentation result by NC; (g) Segmentation result by DRLS; (h) Segmentation result by TSCE; (i) Segmentation result by TSFE; (j) Segmentation result by ITS; (k) Segmentation result by TSME; (l) Segmentation result by Otsu; (m) Segmentation result by EM; (n) Segmentation result by KM; (o) Segmentation result by STS; (p) Segmentation result by FCM.

In addition to composite images, we also use some actual images in practical applications to evaluate the proposed methods and the performance of existing technical methods [31-36]. In the following experiments, we no longer compare normalized segmentation methods because they do not produce meaningful boundaries in these particular applications. In Fig. 2 and Fig. 3, we divided two typical magnetic resonance (MR) ventricular images to demonstrate the superiority of the proposed SD threshold method and the existing method in the segmentation accuracy. Fig. 2 and 3 show the segmentation results of the left ventricle in systole state and diastole state respectively. It can be seen that the SD-threshold method matches the manual segmentation more accurately than all the other state of the art segmentation methods. *Please note that the calibrated parameter N for the MR images is 11.*

We adopt two synthetic datasets and design four quantitative comparison experiments to compare the segmentation effect of proposed methods and state of the art methods. The *Dataset 1* contains 100 images with one bright and dark two types. The mean value of the dark object and the bright object is 100 and 150 respectively. The background average is 50. The noise variance is increased from 1 to 100, and 100 images are generated in the *Dataset 1*. Fig. 4 (a) shows the image produced in *dataset 1* when the variance of noise is 19. *Dataset 2* also contains 100 images with two objects. The difference is that the average of the dark object changes to 80 and the other parameters are the same. Fig. 4 (b) shows the image produced in *dataset 2* when the variance of noise is 19. *Experiment 1* shows segmentation the two objects in *Dataset 1* together and the true boundary is shown in Fig. 4 (c). *Experiment 2* shows segmentation the bright object only in *Dataset 1* and the true boundary is shown in Fig. 4(d). *Experiment 3* shows segmentation the two objects in *Dataset 2* together and the true boundary is shown in Fig. 4 (c). *Experiment 4* shows segmentation the bright object only in *Dataset 2* and the true boundary is shown in Fig. 4 (d).*Because of all the state of the art methods Matlab codes are downloaded, it is very inconvenient to include some methods in the loop to calculate the quantitative results. Therefore, some of these are omitted in quantitative comparison.*

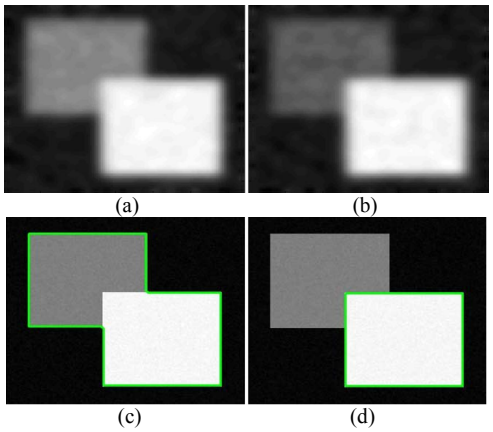

Fig. 4. Illustration of the synthesized images and the designed experiments (a) Synthesized images in *dataset 1*; (b) Synthesized images in *dataset 2*; (c) True boundary in *Experiment 1* and *Experiment 3*; (d) True boundary in *Experiment 2* and *Experiment 4;*

The precision, recall and F-measure are used to assess the performances differences between the proposed SD-threshold method and state of the art methods. For each experiment, some

state of the art methods are better than others and have similar accuracy to the proposed method. However, as with the proposed SD-threshold selection method, none of these experiments performed very well. We show the F-measures drawn in Figs. 5-8. A more detailed comparison is shown in the table. All these results confirm that the proposed SD-threshold method is more accurate than the state of the art in segmenting the different types of images.

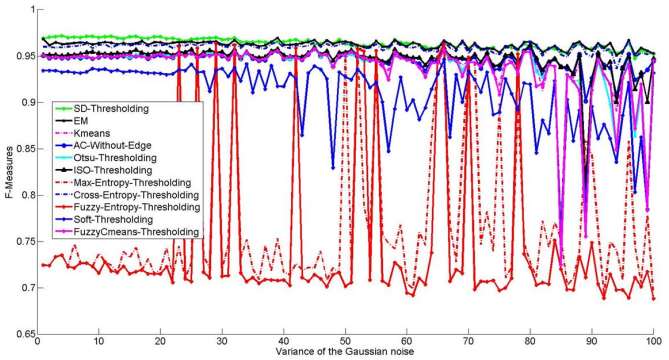

Fig. 5. Plots of F-measures for comparison of the proposed SD-thresholding method and state of the art methods with *Experiment 1*.

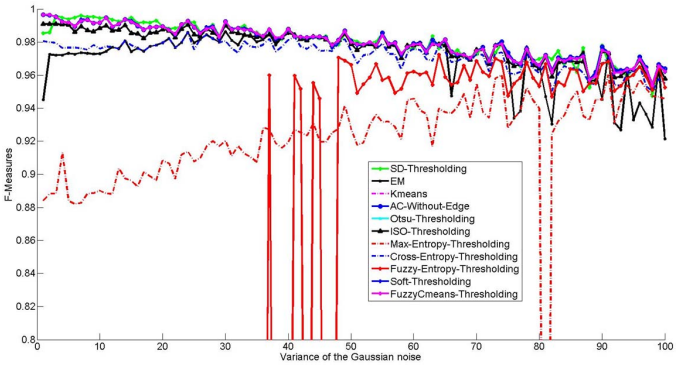

Fig. 6. Plots of F-measures for comparison of the proposed SD-thresholding method and state of the art methods with *Experiment 2*.

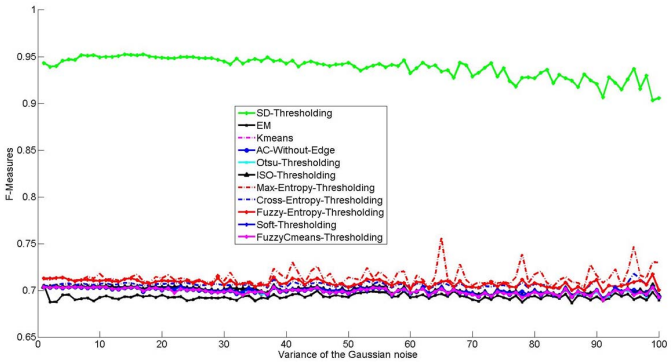

Fig. 7. Plots of F-measures for comparison of the proposed SD-thresholding method and state of the art methods with *Experiment 3*.

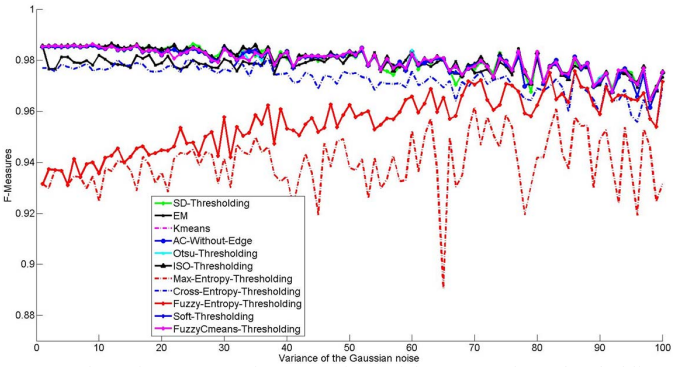

Fig. 8. Plots of F-measures for comparison of the proposed SD-thresholding method and state of the art methods with *Experiment 4*.

IV. Conclusion and Future Work

In this paper, a flexible threshold selection method is proposed to divide the different types of images that are common in practical applications. This threshold selection method is based on the concept of slope differential distribution in this paper. Based on the design of the Fourier transform filter, the slope distribution is calculated from the smooth histogram. Therefore, it can suppress the influence of noise more than state of the art image segmentation method. The method can be calibrated to achieve optimum precision. Therefore, it can meet different segmentation requirements better than state of the art methods in different scenarios. The proposed method can successfully split the object for some failures of the state of the art methods of the evaluation. Use a large number of data sets including composite images and actual images to validate the proposed threshold selection method. The experimental results show that the proposed threshold selection method is much more accurate than the state of the art methods.

References

[1] M. Sezgin and B. Sankur, "Survey over image thresholding techniques andquantitative performance evaluation," *Journal of Electronic Imaging,* vol.13, pp. 146-165, Jan, 2004

[2] C. H. Li and C. K. Lee, ‘‘Minimum cross-entropy thresholding,’’ *Pattern Recogn.* **26**, 617–625, 1993.

[3] H. D. Cheng, Y. H. Chen, and Y. Sun, ‘‘A novel fuzzy entropy approach to image enhancement and thresholding,’’ *Signal Process.* **75**, 277–301, 1999.

[4] T.W. Ridler and S. Calvard "Picture Thresholding using an iterative selection method." *IEEE Trans.Syst. Man Cybern.*8, 630-632, 1978

[5] N. Otsu, "A threshold selection method from gray level histogram," *IEEE Trans.Syst. Man Cybern.* SMC-9, pp.62-66, 1979

[6] T.Y. Li, J.Z. Tsai, R.S. Chang, L.W. Ho and C.F. Yang, “A contrast adjustment thresholding method for surface defect detection based on mesoscopy,”*IEEE Trans. Ind. Inform.* Vol. 11, No. 3, pp. 642-649, 2015

[7] W.V. Aarle, K.J. Batenburg and J. Sijbers, “Threshold selection for segmentation of dense objects in tomograms”, *IEEE Transactions on medical imaging*, Vol. 30(4), pp. 980-989, 2011

[8] K. Yamgar and B.V. Pawar, “Effect of image size on threshold selection for segmentation of dense homogeneous objects in tomographic reconstructions”, *International journal of emerging technology and advanced engineering*, Vol. 4(7), pp. 796-800, 2014

[9] R. Guo and S. M. Pandit, ‘‘Automatic threshold selection based on histogram modes and a discriminant criterion,’’ *Mach. Vision Appl.***10**, 331–338 ~1998.

[10] T. Kurita, N. Otsu and N. Abdelmalek, "Maximum likelihood thresholding based on population mixture models" *Pattern Recogn.* Vol. 25, pp.1231-1240, 1992
[11] F.J. Chang, J.C. Yen and S. Chang, "A new criterion for automatic multilevel thresholding" *IEEE Trans.Image Process*. 4,370-378,1995.
[12] N. Ramesh, J.H. Yoo and I.K. Sethi, "Thresholding based on histogram approximation," *IEE Proc-Vis. Image Signal Process.,* Vol. 142, No. 5, pp.271-279, 1995
[13] G. Moser and S.B. Serpico "Generalized minimum-error thresholding for unsupervised change detection from SAR amplitude imagery." *IEEE Trans.GeoSci Remote Sens.*44(10), 2972-2982, 2006
[14] A. Rosenfeld and P.D. Torre, "Histogram concavity analysis as an aid inthreshold selection," *IEEE Trans. Syst. Man Cybern.* SMC-9, pp. 38-52, 1983
[15] M. E. Yuksel and M. Borlu, "Accurate segmentation of dermoscopic images by image thresholding based on type-2 fuzzy logic," *IEEE Transactions on fuzzy systems*, **17**(4), 976-982 (2009).
[16] M. Pagola, C. Lopez-Molina, J. Fernandez and E. Barrenechea, "Interval type-2 fuzzy sets constructed from several membership functions: application to the fuzzy thresholding algorithm," *IEEE Transactions on fuzzy systems*, **21**(2), 230-244 (2013).
[17] D. T. Anderson, J.C. Bezdek, M. Popescu and J.M. Keller, "Comparing fuzzy, probabilistic and possibilistic partitions," *IEEE Transactions on fuzzy systems*, **18**(5), 906-918 (2010).
[18] S. Aja-Fernandez, A. H. Curiale and G. Vegas-Sanchez-Ferrero, "A local fuzzy thresholding methodology for multi-region image segmentation," *Knowledge-based systems*, **83**, 1-12 (2015)
[19] N.R. Pal, K. Pal, J.M. Keller and J.C. Bezdek, "A possibilistic fuzzy c-means clustering algorithm," *IEEE Transactions on fuzzy systems*, **13**(4), 517-530 (2005).
[20] F. Masulli and S. Rovetta, "Soft transition from probabilistic to possibilistic fuzzy clustering," *IEEE Transactions on fuzzy systems*, **14**(4), 516-527 (2006).
[21] R. Krishnapuram and J.M. Keller, "The possibilistic C-Means Algorithm: insights and recomentations," *IEEE Transactions on fuzzy systems*, **4**(3), 385-393 (1996).
[22] A.M. Bensaid, L.O. Hall, J.C. Bezdek, L.P. Clarke, M.L. Silbiger, J.A. Arrington and R.F. Murtagh, "Validity-Guided (Re)Clustering with application to image segmentation," *IEEE Transactions on fuzzy systems*, **4**(2), 112-123 (1996).
[23] A.P. Dempster, N.M. Laird and D.B. Rubin, "Maximum likelihood from incomplete data via the EM algorithm."*Journal of the Royal Statistical Society, Series B,* Vol. 39,no. 1, pp.1-38, 1977
[24] T. Kanungo, D.M. Mount, N. Netanyahu, C. Piatko, R. Silverman and A.Y. Wu, "An efficient k-means clustering algorithm: analysis and implementation," *Proc. IEEE Conf. Computer Vision and Pattern Recognition,* pp.881–892, 2002.
[25] J. Jiang, J. Liu, H. Qi and Q.H. Dai, "Robust subspace segmentation via nonconvex low rank representation," Information Sciences, Vol. 340, pp. 144-158, 2016.
[26] T.F. Chan and L.A. Vese, "Active contours without edges," *IEEE Transactions on image processing,* Vol.10, No. 2, pp. 266–277, 2001.
[27] S. Lankton and A. Tannenbaum, "Localizing region-based active contours,", *IEEE Transactions on image processing,* Vol.17, No. 11, pp. 2029–2039, 2008.
[28] C. Li, C. Xu, C. Gui and M. D. Fox, "Distance Regularized Level Set Evolution and Its Application to Image Segmentation", IEEE Trans. Image Processing, vol. 19, no.12, pp.3243-3254, 2010.
[29] X. Yang, X. Gao, J. Li, and B. Han, "A shape-initialized and intensity-adaptive level set method for auroral oval segmentation," Information Sciences, vol. 277, pp. 794-807, Sep. 2014.
[30] J.B. Shi and J.Malik, "Normalized cuts and image segmentation,"IEEE transactions on pattern analysis and machine intelligence, vol. 22, no. 8, pp. 888-905, Nov. 2000.
[31] Z.Z. Wang, "A new approach for segmentation and quantitification of cells or nanoparticles", *IEEE T IND INFORM*, Vol. 12, No.3, pp. 962-971, 2016
[32] Z.Z. Wang, "An efficient and robust method for automatically identifying the left ventricular boundary in cine magnetic resonance images", *IEEE T-ASE*, 2016
[33] Z.Z. Wang, "A semi-automatic method for robust and efficient identification of neighboring muscle cells," *Pattern recognition*, Vol. 53, pp. 300-312, 2016
[34] Z.Z. Wang, "Monitoring of GMAW weld pool from the reflected laser lines for real time control", *IEEE T IND INFORM*, Vol. 10, No.4, pp. 2073-2083, 2014
[35] Z.Z. Wang, "Unsupervised recognition and characterization of the reflected laser lines for robotic gas metal arc welding" *IEEE Trans. Ind. Inform.*, Vol. 13, No. 4, pp. 1866-1876, 2017.
[36] Z.Z. Wang, "Automatic segmentation and classification of the reflected laser dots during analytic measurement of mirror surfaces" *Opt Laser Eng*., **83**, 10 (2016).